PHYSICAL REVIEW VOLUME 136, NUMBER 2A 19 OCTOBER 1964

Magnetic Susceptibility of $FeCl_2 \cdot 4H_2O$ from 0.35 to 4.2°K†

J. T. SCHRIEMPF* AND S. A. FRIEDBERG
Carnegie Institute of Technology, Pittsburgh, Pennsylvania

(Received 29 April 1964)

The magnetic susceptibility of $FeCl_2 \cdot 4H_2O$ in powder and single-crystal form has been measured between 0.35 and 4.2°K by an audio-frequency mutual-inductance technique. Temperatures below 2°K were achieved with a liquid He^3 bath. These measurements show $FeCl_2 \cdot 4H_2O$ to be an antiferromagnet with $T_N \sim 1$°K. With the aid of crystallographic evidence, it has been found possible to fit the data in the paramagnetic region with a detailed picture of the lowest spin quintet of the Fe^{++} ion in a monoclinic crystalline field. The same level scheme describes adequately the measured specific heat of the salt in this region. The analysis performed for $T > T_N$ combined with the data for $T < T_N$ suggests that a four-sublattice model may be necessary to interpret in detail the measurements in the ordered state.

INTRODUCTION

THE ground state of the free Fe^{++} ($3d^6$) ion is ^5D. A weak crystalline electric field of sufficiently low symmetry, e.g., rhombic, acting upon this ion completely removes the orbital degeneracy of the ground state, thus "quenching" its orbital angular momentum. Spin-orbit interaction, however, prevents quenching from being quite complete and also lifts the fivefold spin degeneracy left by the crystalline field. Thus the ground state of a ferrous ion in many crystals is expected to consist of a spin quintet which is fully split even in the absence of external fields.

Magnetic measurements on $Fe(NH_4)_2(SO_4)_2 \cdot 6H_2O$ and FeF_2 have been interpreted[1,2] on this basis, the over-all width of the quintet being between 10 and 100 cm^{-1} in both cases. In $Fe(NH_4)_2(SO_4)_2 \cdot 6H_2O$ there is no significant exchange interaction among Fe^{++} ions. In FeF_2, on the other hand, a Néel point has been found[3] near 63°K indicating that the exchange energy is comparable with the zero-field splitting. We shall be concerned in this paper with the properties of $FeCl_2 \cdot 4H_2O$ in which is realized a situation intermediate between these extremes.

Not long ago,[4] the magnetic susceptibility of powdered $FeCl_2 \cdot 4H_2O$ was found to pass through a maximum near 1.6°K. In addition, Curie-Weiss behavior was observed in the liquid-hydrogen range, the Weiss constant θ being of antiferromagnetic sign and equal in magnitude to 2°K. These facts suggested the occurrence of an antiferro-paramagnetic transition in the neighborhood of 1°K. This conclusion was later given support by measurements of the specific heat[5] of the salt. At the lowest temperature achieved, 1.15°K, C_p was found to be rising very rapidly with falling temperature in the way commonly observed just above a cooperative transition point. In addition, a clearly resolved Schottky anomaly was detected having its maximum near 3°K. From the magnitude and location of this maximum, as well as the temperature variation of C_p above the maximum, some general inferences were drawn about the ground state of the Fe^{++} ion. The five basic spin levels appear to be divided into a lower group of two and an upper group of three, all lying within an interval of ~ 10 cm^{-1}. Thus, the exchange energy in $FeCl_2 \cdot 4H_2O$, while large enough to produce cooperative ordering near 1°K, is roughly an order of magnitude smaller than the over-all width of the ground spin quintet.

In view of this fact, it was felt that a study of the single crystal magnetic susceptibilities of $FeCl_2 \cdot 4H_2O$ at liquid He^3 and He^4 temperatures could yield useful information of several kinds. In the paramagnetic region, far enough above the Néel point, one would expect the susceptibilities to reflect in their large anisotropy and temperature variation the details of the ground state of a single Fe^{++} ion. In the analysis of these data, furthermore, an approximate treatment of the relatively small interaction effects might be expected to be adequate. A more precise identification of the Néel point T_N should also emerge from such observations near 1°K. In the antiferromagnetic state, the susceptibilities should indicate the preferred direction of spin orientation and perhaps lend themselves to an analysis giving further details about the exchange interactions. We have, therefore, measured the magnetic susceptibilities of $FeCl_2 \cdot 4H_2O$ between 0.35 and 4.2°K and attempted to extract from the results these various types of information.

EXPERIMENTAL

Single crystals of $FeCl_2 \cdot 4H_2O$ were grown from saturated aqueous solution of the Analytical Reagent Grade material supplied by the Mallinkrodt Chemical

---

† Work supported by the U. S. Office of Naval Research and the National Science Foundation. Brief preliminary accounts of these results have been presented at the Conference on Magnetism and Magnetic Materials, Atlantic City, New Jersey, November 1963 and before the American Physical Society, Philadelphia, Pennsylvania, March 1964 [Bull. Am. Phys. Soc. **9**, 226 (1964)].

* Now at the U. S. Naval Research Laboratory, Washington, D. C.

[1] T. Ohtsuka, H. Abe, and E. Kanda, Science Reports of the Research Institutes, Tohoku University **A9**, 476 (1957).

[2] K. Niira and T. Oguchi, Progr. Theoret. Phys. (Kyoto) **11**, 425 (1954); T. Moriya, K. Motizuki, J. Kanamori, and T. Nagamiya, J. Phys. Soc. Japan **11**, 211 (1956).

[3] J. W. Stout and L. M. Matarrese, Rev. Mod. Phys. **25**, 338 (1953).

[4] R. D. Pierce and S. A. Friedberg, J. Appl. Phys. **32**, 66S (1961).

[5] S. A. Friedberg, A. F. Cohen, and J. H. Schelleng, J. Phys. Soc. Japan **17**, 515 (1962).

Works. The total maximum limit of all impurities was stated by the manufacturer to be less than 0.13 wt %. The principal metallic impurities, Cu and Zn, were present in amounts no greater than 0.005 wt %. It was found that $FeCl_2 \cdot 4H_2O$ was very unstable in the atmosphere; it absorbed water on humid days and became dehydrated on dry days. The resulting contamination was kept to a minimum by harvesting the crystals just before beginning the measurements. They were taken from saturated solution, dried, mounted, and cooled to nitrogen temperatures in a time that was always less than 30 min. Inspection before and after the measurements disclosed no visible contamination in either the powder or crystal specimens. Attempts to coat the crystals with GE7031 cement proved unsatisfactory because the material reacted with the cement and formed what appeared to be a ferric contamination. The measured susceptibilities of coated crystals, which were always significantly higher than those of uncoated samples, will not be reported. Powdered specimens were packed in thin-walled Pyrex spherical containers of 4 to 6 mm diam; specimen masses were of the order of a few tenths of a gram. Single crystal samples, of roughly the same weight, were tied to nylon holders with nylon thread to align them for the measurements; orientations thus established were probably accurate to ±1 to 2 degrees.

The He^3 cryostat and the equipment used to measure the magnetic susceptibilities of these samples have been described elsewhere.[6] An ac mutual induction technique was employed operating generally at a frequency of 500 cps. The calibration substance was powdered $Ce_2Mg_3(NO_3)_{12} \cdot 24H_2O$, which has a susceptibility given by $\chi_p = (0.213 + 2.73/T) \times 10^{-4}$ cgs/g at temperatures down to 0.01°K.[7] This salt was also used as a magnetic thermometer to verify the temperatures obtained from the measured vapor pressures of liquid He^4 (1958 scale)[8] and liquid He^3 (1962 scale).[9] Above 2.0°K the samples were placed in thermal contact with the liquid He^4 by means of He^4 and He^3 transfer gases, while below 2.0°K they were immersed directly in the liquid He^3. The measured susceptibilities were corrected for contributions from the sample holders which were determined in a separate series of experiments.

The reproducibility of the measured susceptibility is, in general, better than ±5%, and the absolute values are probably accurate to ±7 to 8%. The estimated accuracy of the bath temperature is ±0.005°K in the region above, and ±0.01°K in the region below 0.5°K.

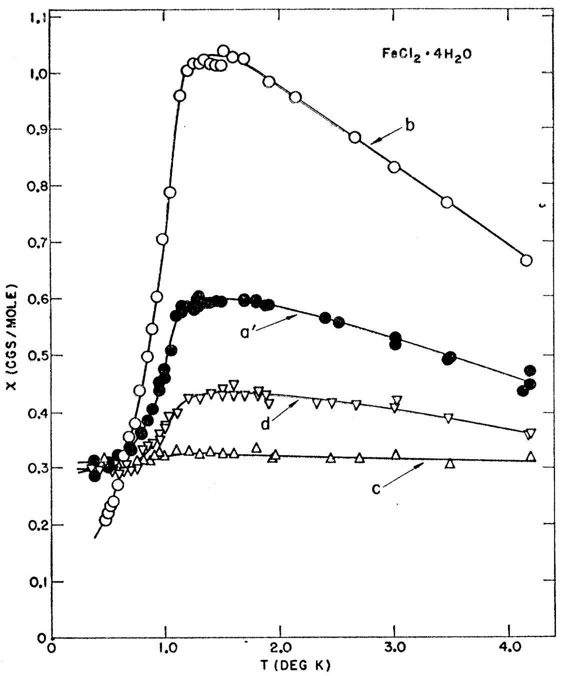

Fig. 1. Crystal susceptibilities of $FeCl_2 \cdot 4H_2O$ as functions of temperature. *b* and *c* are conventional axes of the monoclinic crystal, *a'* is perpendicular to both *b* and *c*, and *d* is at 45° between and in the plane of *a* and *c*. The solid lines are smooth curves drawn through the data.

All susceptibilities, unless otherwise noted, are reported in units of cgs/mole, i.e., emu per mole of magnetic ion.

EXPERIMENTAL RESULTS

Ferrous chloride tetrahydrate forms monoclinic crystals. The typical growth habit described by Groth[10] is indicated in Fig. 3(a). The monoclinic or diad axis is labeled *b* and is perpendicular to the plane containing the axes *a* and *c*, which form an angle $\beta = 112°$[10,11] with one another. Figure 1 shows the results of susceptibility measurements on single crystal specimens of $FeCl_2 \cdot 4H_2O$ between 0.35 and 4.2°K. Open circles represent the values determined with the measuring field parallel to the *b* axis χ_b; triangles represent values of χ_c, while solid circles indicate $\chi_{a'}$, where the a' direction is perpendicular to both *b* and *c*, lies in the *a–c* plane, and deviates from *a* by 22°. Inverted triangles represent values of χ_d, where the direction *d* also lies in the *a–c* plane, making an angle of 45° with the *a* and *c* axes.

These measurements are sufficient to determine fully the susceptibility tensor of the crystal. This tensor has been diagonalized and the principal values determined together with the principal axes *x*, *y*, and *z*. As *b* is the monoclinic axis, it must coincide with one of the principal axes. We arbitrarily let $\chi_b = \chi_z$. The *x* and *y* axes, of course, lie in the *a–c* plane and are orthogonal. We find that the *y* axis makes an angle of $\varphi = 5\frac{1}{2}°$ with

---

[6] J. T. Schriempf and S. A. Friedberg, J. Chem. Phys. **40**, 296 (1964).

[7] J. M. Daniels and F. N. H. Robinson, Phil. Mag. **44**, 630 (1953).

[8] F. G. Brickwedde, H. van Dijk, M. Durieux, J. R. Clement, and J. K. Logan, *The 1958 He^4 Scale of Temperatures* (U. S. Government Printing Office, Washington, 1960), NBS Monograph 10.

[9] S. G. Sydoriak, T. R. Roberts, and R. H. Sherman, *Eighth International Conference on Low Temperature Physics* (Butterworths Scientific Publications, Ltd., London, 1962), p. 297.

[10] P. Groth, Chem. Kryst., **I**, 246 (1906).

[11] B. R. Penfold and J. A. Grigor, Acta Cryst. **12**, 850 (1959).

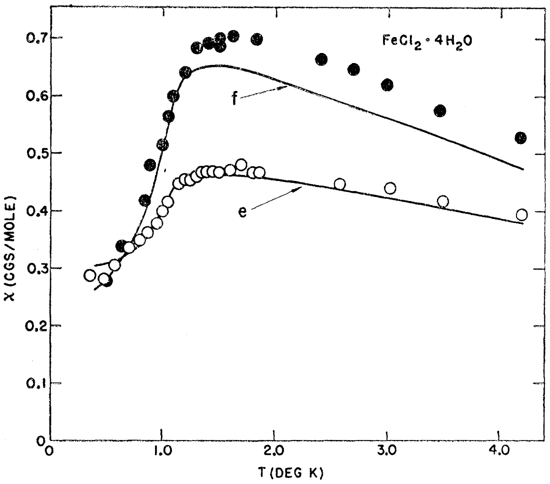

FIG. 2. A comparison of separate measurements of the susceptibility of $FeCl_2 \cdot 4H_2O$ as a function of temperature. The solid lines are calculated from the smooth curves of Fig. 1, while the circles are the direct results of measurements. The solid circles and f indicate powder values, and the open circles and e indicate the susceptibility in the x–y plane at 45° between x and y.

the c direction and an angle of $106\frac{1}{2}°$ with the a direction. The principal-axis calculation depends on differences in the measured values and is thus most accurate where these differences are largest. Between 1.5 and 3.5°K, the above angle $5\frac{1}{2}°$ is obtained with a maximum deviation of $\frac{1}{2}°$. The magnitudes of χ_x and χ_y are, within 1%, essentially those of χ_a, and χ_c, respectively.

A check of the principal axis determination is provided by noting that a measurement of the susceptibility with the magnetic field in the x–y plane and at 45° to the x and y directions should yield one-half the sum of χ_x and χ_y. Data obtained with the field in this direction are plotted as open circles in Fig. 2, together with corresponding values (curve e) calculated from the smooth curves of the above measurements assuming $\varphi = 5\frac{1}{2}°$ at all temperatures. The agreement is quite satisfactory at all but the lowest temperatures, where χ_x and χ_y are nearly equal. In this region, also, the material is no longer paramagnetic so that the symmetry of the susceptibility tensor is no longer assured. Also shown in Fig. 2, in solid circles, are the results of measurements on a powdered specimen of $FeCl_2 \cdot 4H_2O$. The smooth curve f represents the average of the single crystal measurements $\frac{1}{3}(\chi_x + \chi_y + \chi_z)$, and is about 8% lower than the powder measurements, which are in good agreement with those of Pierce and Friedberg.[4] As decomposition of the material resulted in spuriously high susceptibilities in the single-crystal work, the high powder values are felt to be due to the greater instability of the crushed specimens.

As has been stated above, several features of the thermal and powder susceptibility data obtained earlier on $FeCl_2 \cdot 4H_2O$ suggest that it becomes antiferromagnetic near 1°K. The single crystal susceptibilities shown in Fig. 1 are consistent with this conclusion, although they are more complicated than those of the usual antiferromagnet. The source of this complication is the fact that the exchange energy is significantly smaller than the zero-field splitting of the Fe^{++} ion in this material. The large anisotropy evident in the single-crystal susceptibilities above ~1.5°K is not unlike that seen in ferrous salts with negligible exchange interaction at temperatures such that kT is comparable with the zero-field splitting.[12]

In its temperature dependence, $\chi_b(\chi_z)$ resembles the susceptibility of a typical antiferromagnet measured along the direction of preferred spin alignment, although there is some indication that the data taken at the lowest temperatures may extrapolate to a small finite value at 0°K. It appears quite reasonable to identify $\chi_b(\chi_z)$ with $\chi_{\parallel}$, and by so doing we are able to locate the Néel point T_N of $FeCl_2 \cdot 4H_2O$. Fisher[13] has shown that T_N corresponds to the temperature at which $d\chi/dT$ assumes its maximum value. In both the Ising and Heisenberg approximations, Fisher shows this slope actually to be infinite at T_N. Referring to Fig. 1, we see that $d\chi/dT$ could very well be infinite at a temperature of about 1°K, which we take to be T_N. This value is in agreement with the conclusions drawn from specific-heat measurements down to 1.15°K. As we shall see below, it is possible that sublattice canting occurs in this salt, so that the b axis may be the preferred axis only in the sense that the major spin components are spontaneously aligned with it below T_N.

Now consider the behavior of the susceptibility in the a–c plane. In a simple antiferromagnet, $\chi_{\perp}$ would be uniform in that plane and become temperature-independent below T_N. While $\chi_c(\chi_y)$ behaves like $\chi_{\perp}$, $\chi_a(\chi_x)$ is apparently rather different, although at the lowest temperatures its values very nearly coincide with those of χ_c. Thus, considering only data taken well below T_N, one has little difficulty in recognizing perpendicular and parallel susceptibilities. It will be shown that the anisotropy in the a–c plane in the paramagnetic region, as well as the large differences between χ_b and

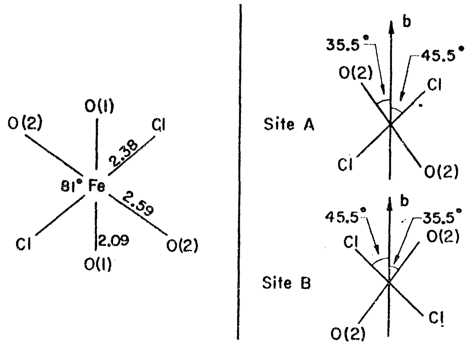

(a) (b)

FIG. 3. Local environment of an Fe^{++} ion in $FeCl_2 \cdot 4H_2O$. Distances are in angstroms. O(1)–O(1) is normal to the plane containing O(2)–O(2) and Cl^-–Cl^-. (b) Local environments of sites A and B projected on the x–z plane in $FeCl_2 \cdot 4H_2O$.

---

[12] For example, $Fe(NH_4)_2(SO_3)_2 \cdot 6H_2O$. (Ref. 1.)

[13] M. E. Fisher, Phil. Mag. 7, 1731 (1962).

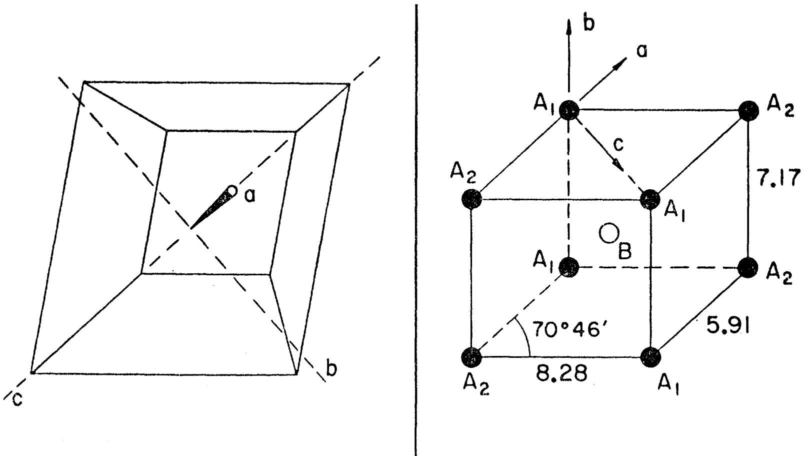

(a) (b)

FIG. 4 (a) View of a single crystal of $FeCl_2 \cdot 4H_2O$ with its b–c plane parallel to the paper. The monoclinic angle is $\beta = 112°$. (b) Body-centered structure of Fe^{++} ions in $FeCl_2 \cdot 4H_2O$. Distances are in angstroms.

the susceptibilities in that plane, are largely the result of the combined effects of the crystalline field and spin-orbit coupling on the complicated ground state of the Fe^{++} ion. In this analysis, however, it becomes quite important that full use be made of the detailed knowledge available on the structure of $FeCl_2 \cdot 4H_2O$. We shall now summarize some of this information.

STRUCTURE OF $FeCl_2 \cdot 4H_2O$

Penfold and Grigor[11] have determined the crystal structure of $FeCl_2 \cdot 4H_2O$. The substance is monoclinic, its space group is $P2_1/c$, and the dimensions of the unit cell are $a = 5.91$ Å, $b = 7.17$ Å, $c = 8.44$ Å with $\beta = 112°10'$. The structure is made up of discrete units consisting of an Fe^{++} ion surrounded by two chloride ions and four water molecules arranged in a distorted octahedron. Two of these groups are found in a unit cell, the Fe^{++} ions occupying inequivalent sites. The basic structural unit is shown in Fig. 3(a). The O(1)–O(1) axis is perpendicular to the plane defined by the O(2)–O(2) and Cl^-–Cl^- axes, which make an angle of 18° with one another. Thus, it is seen that the local environment of the Fe^{++} ion itself possesses monoclinic symmetry with the O(1)–O(1) axis being the local monoclinic axis. Fig. 3(b) indicates the relative orientations of the octahedra about the two inequivalent Fe^{++} ions in the unit cell. In this figure the two octahedra at sites A and B are projected in section on the z–x plane. The direction labeled b is the macroscopic monoclinic axis of the crystal. The local diad axis [O(1)–O(1)] in each complex lies very nearly in the a–c plane, tipping out of that plane by no more than 1°. The two essentially parallel O(1)–O(1) axes at sites A and B deviate from the c direction by an angle of approximately $3\frac{1}{2}$°.

The contents of a unit at site A may be transformed into those at site B by reflection in an a–c plane located at $b/4$ followed by a translation of $c/2$ along c. The angles formed by O(2)–O(2) directions and Cl^-Cl^- directions with the b axis are as shown in Fig. 3 (b). It is interesting to note that the O(1)–O(1) directions deviate from the principal susceptibility axis y by no more than 2°. This fact plays a useful role in the subsesequent analysis. The two sites A and B lie on two interpenetrating lattices and form a body-centered structure as shown in Fig. 4(b), where a B orientation has been chosen for the central ion. Note that the four rectangular faces of the parallelopiped formed by the ions on the A sites are perpendicular to the a–c plane. The central ion has four nearest neighbors, A_1, at 5.54 Å, two second nearest in the a direction at 5.91 Å, four third nearest, A_2, at 6.84 Å, and two fourth nearest neighbors in the b direction at 7.17 Å.

INTERPRETATION OF THE OBSERVATIONS

In attempting a theoretical analysis of the susceptibility of $FeCl_2 \cdot 4H_2O$, we shall concentrate our attention on temperatures far enough above T_N so that the effects of exchange interaction may be taken to be small. In so doing, we are able to treat the observed properties of the salt in terms of the energy levels of a single ferrous ion. The problem of calculating the energy of an Fe^{++} ion in a crystalline environment of low symmetry has been discussed by Tinkham.[14] He allows the crystalline field to have rhombic symmetry so that the ground state of the ion in this field is not orbitally degenerate. A spin Hamiltonian is assumed to be of the form

$$\mathcal{H} = D[S_{z'}^2 - \tfrac{1}{3}S(S+1)] + E(S_{x'}^2 - S_{y'}^2) + \mu_B(g_{x'}H_{x'}S_{x'} + g_{y'}H_{y'}S_{y'} + g_{z'}H_{z'}S_{z'}) , \quad (1)$$

where x', y', and z' are the principal axes of the crystalline field at the ion, μ_B is the Bohr magneton, $\mathbf{H}$ the applied field, $\mathbf{S}$ the spin of the Fe^{++} ion, $g_{x',y',z'}$ the diagonal elements of the spectroscopic splitting factor, and D and E are constants. Note that the second-order Zeeman term has been omitted here because its effect will prove negligible in the temperature range of interest. Taking the spin of the Fe^{++} ion to be its true value, $\mathbf{S} = 2$, we may obtain the eigenvalues of this Hamiltonian for

---

[14] M. Tinkham, Proc. Roy. Soc. **A236**, 535 (1956).

$\mathbf{H}=0$:

$$W_1=D(4+12E^2/D^2)^{1/2}, \tag{2a}$$

$$W_2=2D, \tag{2b}$$

$$W_3=-D+3E, \tag{2c}$$

$$W_4=-D-3E, \tag{2d}$$

$$W_5=-D(4+12E^2/D^2)^{1/2}. \tag{2e}$$

The corresponding eigenfunctions are found to be

$$\varphi_1=(\cos\alpha/\sqrt{2})[|2\rangle+|-2\rangle]+\sin\alpha|0\rangle, \tag{3a}$$

$$\varphi_2=(1/\sqrt{2})[|2\rangle-|-2\rangle], \tag{3b}$$

$$\varphi_3=(1/\sqrt{2})[|1\rangle+|-1\rangle], \tag{3c}$$

$$\varphi_4=(1/\sqrt{2})[|1\rangle-|-1\rangle], \tag{3d}$$

$$\varphi_5=\cos\alpha|0\rangle-(\sin\alpha/\sqrt{2})[|2\rangle+|-2\rangle], \tag{3e}$$

where

$$\tan\alpha=\frac{\sqrt{3}E/D}{1+(1+3E^2/D^2)^{1/2}}. \tag{3f}$$

Since our spin Hamiltonian contains no terms in $\mathbf{S}$ higher than second order, we may use these results in a discussion of the Fe^{++} ion in a crystalline field of monoclinic symmetry, as occurs in $\mathrm{FeCl_2\cdot 4H_2O}$. It is important to note, however, that only one of the principal axes, x', y', z', need coincide with a simple axis of the monoclinic structural unit. This simple axis will be the local diad axis (in our case O(1)–O(1)), which we label z' and arbitrarily choose as the axis of quantization. The other two principal axes of the crystalline field, x' and y', are orthogonal and must lie in the plane determined, in our problem, by the O(2)–O(2) and $\mathrm{Cl^-}-\mathrm{Cl^-}$ directions.

Our choice of the above formalism with $\mathbf{S}$ equal to the free-ion spin value of 2 is supported by recent spectroscopic results on the salt $\mathrm{CrCl_2\cdot 4H_2O}$.[15] This salt has been shown to be isostructural with $\mathrm{FeCl_2\cdot 4H_2O}$. The details of the local environment of the chromous ion are remarkably similar to those found in the ferrous case. The largest difference is found in the M^{++} $-$O(2) distance, which for the chromous salt is 2.80 Å as opposed to 2.59 Å in the ferrous case. The measured optical absorption bands indicate that in $\mathrm{CrCl_2\cdot 4H_2O}$ the crystalline field at the Cr^{++} ion is of sufficiently low symmetry to remove completely the fivefold orbital degeneracy of the ^5D free-ion ground state. Since the levels arising from the ^5D free-ion ground state of Fe^{++} in essentially the same crystalline field should present a similar but inverted pattern to that found for Cr^{++}, we may expect Fe^{++} in $\mathrm{FeCl_2\cdot 4H_2O}$ to have an orbitally nondegenerate ground state. Thus, it is reasonable to employ a spin Hamiltonian formalism with $\mathbf{S}$ the true spin.

We now calculate the paramagnetic susceptibility of the Fe^{++} ion relative to the local set of principal axes. This has been done using Van Vleck's formula.[16] One assumes that an energy state E_j of an ion can be developed in powers of the applied magnetic field H,

$$E_j=E_j^{(0)}+E_j^{(1)}H+E_j^{(2)}H^2+\cdots. \tag{4}$$

If the field is in, say, the z' direction, the susceptibility in that direction may be shown to be

$$\chi_{z'}'=\frac{\sum_j \exp(-E_j^{(0)}/kT)[E_j^{(1)2}/kT-2E_j^{(2)}]}{\sum_j \exp(-E_j^{(0)}/kT)}. \tag{5}$$

In applying this formula we have taken as $E_j^{(0)}$, the zero-field eigenvalues, Eqs. (2), of the spin Hamiltonian, Eq. (1). The Zeeman term has then been treated as a perturbation using as zeroth-order wave functions the zero-field eigenfunctions, Eqs. (3), of the spin Hamiltonian. The summation in Eq. (5) has been taken over the five levels of the lowest spin multiplet. In this treatment the influence of higher orbital states has been included to the extent that they appear in the perturbation calculation of which the effective spin Hamiltonian is the result.

Using this technique one finds the paramagnetic susceptibility per ion to be, for $\mathbf{H}\rightarrow 0$,

$$\chi_{z'}'=(-2g_{z'}^2\mu_B^2/Z)\{C_1e^{-w_1/kT}+(C_2-C_1)e^{-w_2/kT}+C_3(e^{-w_3/kT}-e^{-w_4/kT})-C_2e^{-w_5/kT}\}, \tag{6a}$$

where

$$Z=e^{-w_1/kT}+e^{-w_2/kT}+e^{-w_3/kT}+e^{-w_4/kT}+e^{-w_5/kT}, \tag{6b}$$

$$C_1=\frac{4D^2+6E^2+2D(4D^2+12E^2)^{1/2}}{3DE^2(4+12E^2/D^2)^{1/2}}, \tag{6c}$$

$$C_2=\frac{6E^2/D}{4D^2+12E^2+(2D^2+3E^2)(4+12E^2/D^2)^{1/2}}, \tag{6d}$$

$$C_3=1/6E. \tag{6e}$$

In order to obtain the susceptibility in the y' and z' directions, it is necessary to transform from one principal axis to another. The transformation from z' to y' is accomplished[17] by replacing D by $-\frac{1}{2}(D+3E)$, E by $\frac{1}{2}$ $(D-E)$, and $g_{z'}$ by $g_{y'}$ wherever they appear. i.e., in $C_{1,2,3}$ and $W_{1,2,3,4,5}$. Similarly, one transforms from z' to x' by replacing D by $\frac{1}{2}$ $(3E-D)$, E by $-\frac{1}{2}$ $(D+E)$, and $g_{z'}$ by $g_{y'}$.

These expressions can be readily modified to include the effects of weak exchange in a simplified molecular-field approximation.[18] This approximation consists of the addition to the spin Hamiltonian for a single ion,

---

[15] W. A. Runciman and R. W. G. Syme, Phil. Mag. 8, 605 (1963).

[16] J. H. Van Vleck, *The Theory of Electric and Magnetic Susceptibilities* (Oxford University Press, London, 1932), p. 181.

[17] K. D. Bowers and J. Owen, Rept. Progr. Phys. 18, 321 (1955).

[18] See, for example, T. Moriya, K. Motizuki, J. Kanamori, and T. Nagamiya, J. Phys. Soc. Japan 11, 211 (1956).

Eq. (1), a term of the form $A\langle\delta\mathbf{S}\rangle\cdot\mathbf{S}$. A is a constant, and, if only interaction with z equivalent neighbors is considered, it may be written $A=2zJ$, where J is the exchange integral. This amounts to adding to the applied field acting on a single ion an effective exchange field defined by

$$(H_{\text{ex}})_{x'}=-(A/g_{x'}{}^2\mu_{\text{B}}{}^2)\chi_{x'}H_{x'}\,, \tag{7a}$$

$$(H_{\text{ex}})_{y'}=-(A/g_{y'}{}^2\mu_{\text{B}}{}^2)\chi_{y'}H_{y'}\,, \tag{7b}$$

$$(H_{\text{ex}})_{z'}=-(A/g_{z'}{}^2\mu_{\text{B}}{}^2)\chi_{z'}H_{z'}\,, \tag{7c}$$

where $\chi_{x',y',z'}$ are the components of the net ionic susceptibility. Now the magnetic moment is taken to be due to the paramagnetic response of the ions to the total effective field, i.e.,

$$M_{x'}=\chi_{x'}'[H_{x'}+(H_{\text{ex}})_{x'}]\,, \tag{8}$$

with similar expression for M_y and M_z.

The susceptibility parallel to x' is, of course, defined by

$$\chi_{x'}=\lim_{H_{x'}\to 0}\frac{M_{x'}}{H_{x'}}\,; \tag{9}$$

and upon combining Eqs. (7), (8), and (9) one has

$$\chi_{x'}=\frac{\chi_{x'}'}{1+(A/g_{x'}{}^2\mu_{\text{B}}{}^2)}\,. \tag{10}$$

Similar equations can be written for $\chi_{y'}$ and $\chi_{z'}$.

In the high-temperature limit, these expressions assume the following simple forms:

$$\chi_{z'}=\frac{2g_{z'}{}^2\mu_{\text{B}}{}^2/k}{T+(7/5)(D/k)+2A/k}\,, \tag{11a}$$

$$\chi_{x'}=\frac{2g_{x'}{}^2\mu_{\text{B}}{}^2/k}{T-(7/10)[(D-3E)/k]+(2A/k)}\,, \tag{11b}$$

$$\chi_{y'}=\frac{2g_{y'}{}^2\mu_{\text{B}}{}^2/k}{T-(7/10)[(D+3E)/k]+(2A/k)}\,. \tag{11c}$$

It should be noted that, although the Fe^{++} ions in $FeCl_2\cdot 4H_2O$ are distributed over inequivalent sites of two types, the powder susceptibility in the paramagnetic region will always simply be $\frac{1}{3}(\chi_{x'}+\chi_{y'}+\chi_{z'})$. This follows from the fact that the local environment at an A site is the mirror image of that at a B site, and we have included exchange only in a molecular-field approximation, in which the possible inequivalence of significantly interacting ions is ignored. In the high-temperature limit, assuming an isotropic splitting factor, one obtains for the powder susceptibility

$$\chi_p=\frac{2g^2\mu_{\text{B}}{}^2/k}{T+2A/k}\,, \tag{12}$$

where $g=g_x=g_y=g_z$. We recall that in the hydrogen region Pierce and Friedberg[4] were able to fit their powder data with a Curie-Weiss law using $g=2.19$ and $\theta=2°\text{K}$. In addition, preliminary single-crystal measurements at these temperatures by R. Pierce indicate that the splitting factor is nearly isotropic. The theoretical result for χ_p just given shows that the Weiss constant is essentially of exchange origin and gives us the value $A=1.0k$. An exchange constant of this magnitude is quite consistent with the value cited earlier for the Néel temperature, $T_N\approx 1°\text{K}$.

The structure data[11] show that the environments of the two ions in a unit cell are related by a mirror reflection in the a–c plane (followed by translation along c); thus the fields at the two sites must have mirror symmetry. The axes for sites A and B have been defined above to have this mirror symmetry, and thus for one-half the ions the axes are right-handed, while for the other half they are left-handed. The spin Hamiltonian is unaffected by a transformation from one type of site to the other. Thus, the same constants D,E, and g will apply to all Fe^{++} ions in the crystal.

Having calculated the paramagnetic susceptibility of an Fe^{++} ion with respect to the principal axes of its own crystalline field, we now turn to the problem of calculating the susceptibility of a macroscopic single-crystal sample. As noted above, the local axis z' at either an A or a B site is very nearly parallel to the macroscopic principal axis y. We shall assume them to be coincident and write

$$\chi_{z'}=\chi_y\,. \tag{13a}$$

Since local axes y' and x' have not yet been completely fixed relative to the crystalline structure, let us say that x' at each site makes an angle of θ with the b axis measured toward the appropriate O(2)–O(2) direction [see Fig. 3(b)]. x', of course, lies in the plane containing O(2) and Cl^- ions, and y' is orthogonal to x' and z'. Noting that the macroscopic z–x plane is essentially parallel to each x'–y' plane, we may complete the set of transformation relations:

$$\chi_z=\chi_{x'}\cos^2\theta+\chi_{y'}\sin^2\theta\,, \tag{13b}$$

$$\chi_x=\chi_{y'}\cos^2\theta+\chi_{x'}\sin^2\theta. \tag{13c}$$

In Eqs. (13) the susceptibility has been assumed to be in units of cgs/mole. As was noted earlier, while χ_z is precisely χ_b, the magnitudes of χ_x and χ_y are very nearly equal to those of $\chi_{a'}$ and χ_c, respectively.

It should be emphasized that, because the symmetry of the crystalline field at a given Fe^{++} site is only monoclinic, the correct value of the angle θ in the above transformation is not obvious from structural considerations alone. Our eventual choice of θ will be such as to optimize the fitting of theoretical expressions to single-crystal susceptibility data. It should be noted, however, that at least two choices, $\theta=\pm 45°$, are rather clearly excluded. $\theta=+45°$ would correspond to the identification of the x' direction with the Cl^-–Cl^- axis. Looking at the transformation equations [Eqs. (13)], we see that for $\theta=45°$ one expects the susceptibility to be isotropic in the macroscopic z–x plane. The data

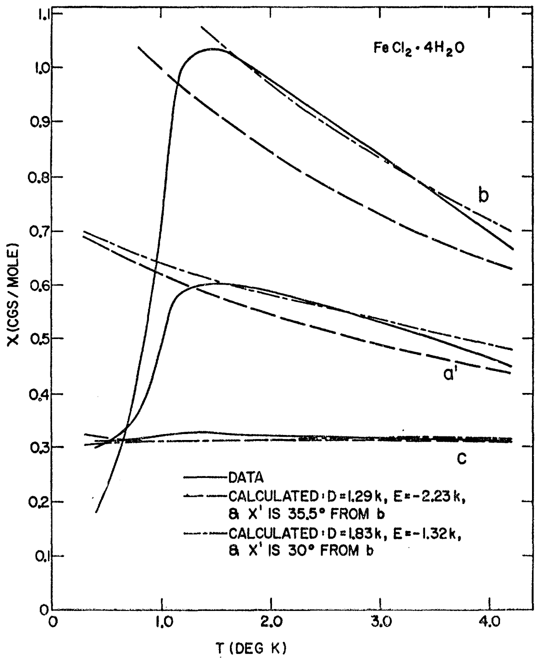

FIG. 5. A comparison between calculated and measured crystalline susceptibilities of FeCl$_2$·4H$_2$O. The solid lines are reproduced from Fig. 1, while the broken lines are calculated as described in the text.

(χ_b and $\chi_{a'}$ in Fig. 1), however, exhibit strong anisotropy in this plane at all temperatures in the paramagnetic region.

The determination of a suitable value of θ as well as the selection of the constants D and E appearing in the spin Hamiltonian have been carried out by a trial-and-error procedure. This process has been greatly facilitated by the rapid computation of susceptibilities as functions of temperature made possible by the CIT Bendix G-20 computing facility. Initially, the spectroscopic splitting factor was assumed isotropic and equal to the powder value determined at hydrogen temperatures, $g=2.19$. Exchange was included in the molecular field approximation described above. The exchange constant, $A=1.0\ k$, was obtained from the Weiss constant needed to describe the hydrogen temperature powder data. Preliminary values of θ, D, and E giving the best agreement with the measured susceptibilities were then calculated.

A final improvement in the fitting of the data was obtained by allowing the splitting factor to be anisotropic. Using the perturbation expressions[19] for D, E, and $g_{x',y',z'}$, and the assumption $g\approx\frac{1}{3}(g_{x'}+g_{y'}+g_{z'})$, one finds

$$g_{x'}=g+(2D/3\lambda)-(2E/\lambda)\,, \tag{14a}$$

$$g_{y'}=g+(2D/3\lambda)+(2E/\lambda)\,, \tag{14b}$$

$$g_{z'}=g-(4D/3\lambda)\,. \tag{14c}$$

We have taken the spin-orbit constant λ to have its free-ion value,[20] $\lambda=-100$ cm^{-1}. The splitting factors obtained using provisional values of D and E are $g_{x'}=2.16$, $g_{y'}=2.20$, and $g_{z'}=2.21$. The anisotropy is small enough to justify the approximation $g\approx\frac{1}{3}(g_{x'}+g_{y'}+g_{z'})$ to the exact relation $g=[\frac{1}{3}(g_{x'}^2+g_{y'}^2+g_{z'}^2)]^{1/2}$ as well as the above use of Eq. (12) to obtain the value of A. These splitting factors are consistent with the preliminary single-crystal results obtained by Pierce in the hydrogen range.

At this point, it is appropriate to justify the fact that we have ignored the second-order Zeeman term $-\frac{1}{2}(\alpha_{x'}H_{x'}^2+\alpha_{y'}H_{y'}^2+\alpha_{z'}H_{z'}^2)$ in our spin Hamiltonian. Using again the perturbation expressions for $g_{x',y',z'}$ plus those[19] for $\alpha_{x',y',z'}$, one finds corrections to the ionic susceptibility such as

$$\chi_{x'_0}=\alpha_{x'}=(2\mu_B^2/\lambda)[1-(g_{x'}/2)]\approx 2\times10^{-3}\mu_B^2. \tag{15}$$

The temperature-independent Van Vleck susceptibility arising from the terms in α in the spin Hamiltonian is thus roughly three orders-of-magnitude smaller than the temperature-dependent contributions calculated in the helium region.

Having accounted for the anisotropy of the splitting factors by inserting Eqs. (14) into the susceptibility expressions, new values of D and E can be obtained for each θ chosen. It was found possible to adjust D and E to produce a good fit of all three susceptibilities above 1.5°K at $\theta=30°$. Figure 5 shows the experimental susceptibility curves (solid lines) together with the fitted theoretical curves for $\theta=30°$, $D=1.83\ k$, and $E=-1.32\ k$. The values of the splitting factors are those given above, and D and E are not significantly different from the provisional values used in their calculation. It will be seen that the agreement is quite satisfactory in the paramagnetic region but fails, as expected, in the immediate vicinity of the Néel point and below. Also shown on the same diagram are the best theoretical curves obtainable for $\theta=35.5°$, corresponding to the artificial assumption that the crystalline-field principal axis x' coincides with the O(2)−O(2) direction in the octahedral complex. Note that, while reasonable agreement with values of χ_c is possible, the discrepancies are much larger for $\chi_{a'}$ and χ_b.

It is appropriate to ask whether the value $\theta=30°$ is reasonable on general physical grounds. Adopting a simple ionic model of the octahedral complex in which each Cl$^-$ ion is replaced by a point charge of magnitude $-|e|$ and each H$_2$O by a point dipole, an estimate of the location of these axes is possible. The electrostatic potential at a point is expanded to terms of second order in the coordinates and then cross terms eliminated by transformation to what we have called the system of principal axes. A calculation of this type performed by M. Amitay of this laboratory actually yields

---

[19] See, for example, M. H. L. Pryce, Nuovo Cimento Suppl. **6**, 817 (1957).

[20] B. Bleaney and K. W. H. Stevens, Rept. Progr. Phys. **16**, 108 (1953).

$\theta = 30°$. The precise agreement with the value deduced in the fitting of the data is probably fortuitous but at least suggests that the angle chosen is not physically unreasonable.

Let us consider now the lowest spin-multiplet energy levels of a single Fe^{++} ion implied by the fitting of the paramagnetic susceptibility data. We have found $D = 1.83\ k$ and $E = -1.32\ k$. Substituting these parameters into the expressions for the eigenvalues of the spin Hamiltonian in zero external field, we obtain the energies indicated in Fig. 6.

The five spin levels are seen to be fully split, as would be expected from the fact that E is quite different from zero. It is significant, however, that they are grouped roughly into a lowest doublet, an intermediate doublet, and a single upper level. From Eqs. (2) it will be seen that such a level sequence could also be obtained with a negative value of D ($-2.895\ k$) and a small but nonzero E ($-0.255\ k$). This implies that the spin Hamiltonian would have more nearly axial symmetry about some direction other than the one arbitrarily chosen as the axis of quantization. That this direction is the x' axis follows from the fact that our fitting of the data requires $D > 0$ and $E < 0$. For some purposes it might be useful to take the axis of quantization as x', although we shall not do so in the present calculation. Following such a transformation, the five levels reading from bottom to top would be associated with the eigenfunctions ϕ_1 through ϕ_5 in the order given in Eqs. (3).

Our picture of the lowest spin quintet bears some qualitative resemblance to that used by Ohtsuka *et al.*,[1] to describe the magnetic and thermal properties of $Fe(NH_4)_2\ (SO_4)_2 \cdot 6H_2O$. There, too, the five levels could be described roughly as a lower split doublet and an upper group of three nondegenerate levels. The splittings in the case of the Tutton salt, however, are much larger, the doublet separation being 6.4 cm^{-1} and the over-all width amounting to about 71 cm^{-1}. This difference appears to be associated with the fact that the octahedral complex in $FeCl_2 \cdot 4H_2O$ departs much more severely from cubic symmetry than in the Tutton salt, where the octahedral complex consists of an Fe^{++} ion surrounded by six H_2O's at distances of roughly 2.1 Å. This probably causes a greater splitting of the components of the state $^5T_2$ in $FeCl_2 \cdot 4H_2O$. Since the width of the basic spin quintet is of the order of $\lambda^2/$(orbital splitting), the somewhat reduced width in the chloride is reasonable. One consequence of the closer spacing of the ground-state components in this salt is the possibility of observing paramagnetic resonance absorption with conventional equipment, something which cannot be done with $Fe(NH_4)_2$ $(SO_4)_2 \cdot 6H_2O$. Experiments of this type are in progress.

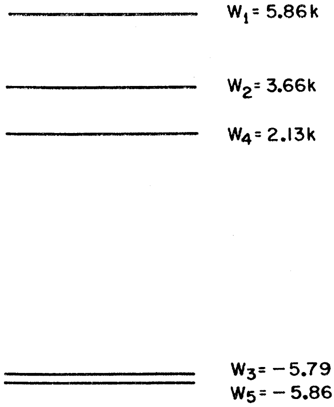

FIG. 6. Energy-level scheme obtained by fitting the data as described in the text. These separations are a result of $D = 1.83\ k$ and $E = -1.32\ k$, with $\theta = 30°$.

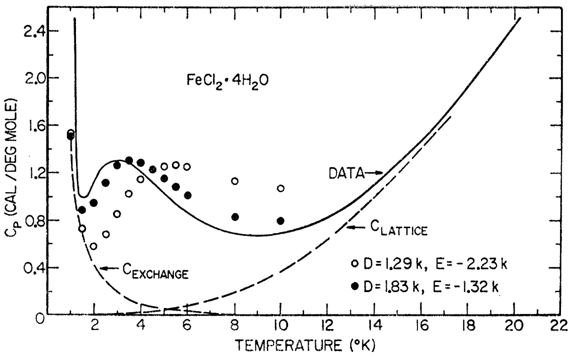

FIG. 7. Specific heat of $FeCl_2 \cdot 4H_2O$ as a function of temperature. The solid line indicates the results of measurements by Friedberg, Cohen, and Schelleng. Open circles represent values calculated as discussed in the text with $\theta = 35.5°$, while solid circles are obtained with $\theta = 30°$.

The specific heat of $FeCl_2 \cdot 4H_2O$ has been measured[5] between 1.15 and 20°K and exhibits a clearly resolved Schottky anomaly, which has a maximum near 3°K. It was possible to describe several features of that anomaly; namely, the temperature of the maximum, and the magnitude of the maximum, in a semiquantitative way by assuming the Fe^{++} ground state to consist of a lower doublet and upper triplet with a mean separation of 8.3 k. It is significant that the detailed level scheme deduced from the susceptibility results has roughly these characteristics. It is important, therefore, that we compute the single-ion contribution to the specific heat from this level scheme and compare the results with the specific-heat data.

We may write the single-ion heat capacity as

$$C_{\text{ion}} = \frac{R}{T^2}\left[\sum_{n=1}^{5} W_n^2 e^{-W_n/kT} \Big/ \sum_{n=1}^{5} e^{-W_n/kT} - \left(\sum_{n=1}^{5} W_n e^{-W_n/kT} \Big/ \sum_{n=1}^{5} e^{-W_n/kT}\right)^2\right\}, \quad (16)$$

where the W_n are as previously defined. To this we must add the lattice contribution already deduced from the experimental data and valid up to about 15°K; namely, $C_{\text{lattice}}/R = 1.78 \times 10^{-4} T^3$. This does not complete the picture, however. A cooperative anomaly is expected at the Néel point. As is seen in Fig. 7 (solid curve), the experimental data reveal the high-temperature side of this anomaly. Were it not for the Schottky bump, the lambda anomaly would probably exhibit the typical "tail" for $T > T_N$ associated with the gradual diminution of short-range order with rising temperature. This additional heat capacity, which results from exchange interactions among Fe^{++} ions, must be estimated and added to the Schottky anomaly, a single-ion effect, and the lattice heat capacity. In the absence of any applicable general theory of this exchange contribution we shall assume it to be roughly of the form $C_{\text{exchange}} = \text{const}/T^2$. The constant was taken to be $0.75R$, a value which yields reasonable agreement between measured and calculated total heat capacities at the maximum in the Schottky anomaly.

In Fig. 7 the solid dots represent the sum, $C_{\text{ion}} + C_{\text{lattice}} + C_{\text{exchange}}$, where C_{ion} has been calculated using the best values for D and E corresponding to $\theta = 30°$. The agreement with the measured values is satisfactory. Open circles in the same figure represent the same quantities, where now C_{ion} has been computed using the parameters required by the assumption $\theta = 35.5°$. These results are clearly in much greater disagreement with the data than those corresponding to $\theta = 30°$. In view of the difficulty in estimating C_{exchange}, it is probably not worthwhile to attempt to improve the fit of the specific-heat data by further adjustment of parameters.

We have seen that it is possible, by treating $FeCl_2 \cdot 4H_2O$ as a system of independent Fe^{++} ions coupled weakly by exchange interactions, to account in a reasonable way for single-crystal susceptibilities and the specific heat in the region above the Néel point. To extend the theory to the region below T_N, one must treat in some way the cooperative transition at T_N and eventually adopt a proper approach to the problem of a strongly coupled and highly ordered spin system near the absolute zero. This program proves to be a formidable one and has not been carried out. Certain qualitative observations, however, can be made which have a bearing on the problem of $FeCl_2 \cdot 4H_2O$ in the antiferromagnetic state. We notice first of all that the coefficient D of the single-ion spin Hamiltonian is positive for our choice of local axes. This means that the crystalline field encourages the Fe^{++} moment to orient itself in the plane perpendicular to the z' axis. At the same time, the coefficient E is negative, making it energetically favorable for the Fe^{++} moment to approach the x' direction. The macroscopic b axis is parallel to the x'–y' plane and closest to the x' direction. It is the b axis, of course, which appears to be the preferred axis of spin alignment in the antiferromagnetic state. Single-ion anisotropy, however, favors canting of Fe^{++} moments away from the b axis.

We have seen from the paramagnetic data that isotropic antiferromagnetic exchange of the form $J\mathbf{S}_1 \cdot \mathbf{S}_2$ probably acts between neighbors. Furthermore, the exchange integral J deduced from the high-temperature Weiss constant is of the proper magnitude to produce cooperative ordering of the spin system near 1°K. However, it is quite possible that this is not the only type of exchange coupling between neighboring Fe^{++} ions. Referring to the crystallographic data, one finds that the midpoint of the line connecting the two ions in a unit cell is not a center of inversion. Moriya[21] has pointed out that, under these circumstances, an anisotropic superexchange coupling of the Dzialoshinski-Moriya type, that is, of the form $\mathbf{D} \cdot \mathbf{S}_1 \times \mathbf{S}_2$, may exist. He further shows that $\mathbf{D} \approx (\Delta g/g)J$. In our case, $\Delta g/g$ is about 10% so that this interaction may not be completely negligible. Its effect is to cause coupled neighboring spins to deviate from the strict antiparallelism favored by the ordinary isotropic exchange. Were the antiferromagnetic spin system to be subdivided into two sublattices, since both the single-ion anisotropy and the anisotropic superexchange would favor sublattice canting, a weak ferromagnetic moment should appear in some direction. Moriya[22] has also shown that the susceptibility of a weak ferromagnet should deviate from the high-temperature Curie-Weiss law in a characteristic way as the Néel temperature is approached. $FeCl_2 \cdot 4H_2O$ does not exhibit this kind of deviation, nor does it give any evidence of a spontaneous ferromagnetic moment at or below the Néel point. It appears, therefore, that a two sublattice model is not realistic in this case.

Moriya[21] has shown in his discussion of the spin arrangement in $CuCl_2 \cdot 2H_2O$ that, by allowing the spins to occupy sites on four sublattices, it is possible to have canting of individual spins away from the preferred axis but at the same time no net spontaneous ferromagnetic moment. In the case of $FeCl_2 \cdot 4H_2O$ it seems quite reasonable that such spin canting does indeed exist, for both the anisotropic super-exchange and the strong single ion anisotropy favor spin alignment at some angle to the b axis. Thus even a molecular-field treatment of the antiferromagnetic state of this compound becomes rather involved. This problem will be treated by Dr. N. Uryû in a later publication.

ACKNOWLEDGMENTS

The authors are grateful to Dr. T. Oguchi for many helpful discussions concerning the theoretical part of this investigation, and to R. Pierce for permission to use his unpublished crystal susceptibility data for $FeCl_2 \cdot 4H_2O$ at hydrogen temperatures.

---

[21] T. Moriya, Phys. Rev. **120**, 91 (1960).

[22] T. Moriya, Phys. Rev. **117**, 635 (1960).